

# LOAN DOCUMENT

DTIC ACCESSION NUMBER	PHOTOGRAPH THIS SHEET	INVENTORY				
	LEVEL					
	<div style="border: 1px solid black; padding: 5px; display: inline-block;">WL-TR-96-2097</div> DOCUMENT IDENTIFICATION					
<div style="border: 1px solid black; padding: 10px; display: inline-block;"><b>DISTRIBUTION STATEMENT A</b> Approved for public release Distribution Unlimited</div>						
DISTRIBUTION STATEMENT						
<div style="border: 1px solid black; padding: 5px;"><small>ACCESSION FOR</small> NTIS <input type="checkbox"/> GRA&amp;I <input checked="" type="checkbox"/> DTIC <input type="checkbox"/> TRAC <input type="checkbox"/> UNANNOUNCED <input type="checkbox"/> JUSTIFICATION <input type="checkbox"/>  <small>BY</small>  <small>DISTRIBUTION/</small>  <small>AVAILABILITY CODES</small> <table border="1" style="width: 100%; border-collapse: collapse;"><tr><td style="width: 50%;"><small>DISTRIBUTION</small></td><td style="width: 50%;"><small>AVAILABILITY AND/OR SPECIAL</small></td></tr><tr><td style="height: 40px; vertical-align: bottom;">A-1</td><td></td></tr></table></div>	<small>DISTRIBUTION</small>	<small>AVAILABILITY AND/OR SPECIAL</small>	A-1		<div style="border: 1px solid black; height: 150px; margin-bottom: 10px;"></div> DATE ACCESSIONED <div style="border: 1px solid black; height: 100px; margin-bottom: 10px;"></div> DATE RETURNED <div style="border: 1px solid black; height: 100px;"></div> REGISTERED OR CERTIFIED NUMBER	
<small>DISTRIBUTION</small>	<small>AVAILABILITY AND/OR SPECIAL</small>					
A-1						
<div style="border: 1px solid black; padding: 10px; display: inline-block;">A-1 19960812 159</div> DATE RECEIVED IN DTIC						
PHOTOGRAPH THIS SHEET AND RETURN TO DTIC-FDAC						

H  
A  
N  
D  
L  
E  
  
W  
I  
T  
H  
  
C  
A  
R  
E

**WL-TR-96-2097**

**THE EFFECT OF HIGH FREESTREAM  
TURBULENCE ON FILM COOLING  
EFFECTIVENESS**



**Jeffrey P. Bons  
Richard B. Rivir  
Charles D. Mac Arthur**

**13-16 JUNE 1994**

**FINAL REPORT 1 NOVEMBER 1995--9 JULY 1996**

**Approved for public release; distribution unlimited**

**AERO PROPULSION & POWER DIRECTORATE  
WRIGHT LABORATORY  
AIR FORCE MATERIEL COMMAND  
WRIGHT-PATTERSON AIR FORCE BASE, OH 45433-7650**

**This paper is declared a work of the U.S. Government and as such is not subject to copyright protection in the United States**

# NOTICE

WHEN GOVERNMENT DRAWINGS, SPECIFICATIONS, OR OTHER DATA ARE USED FOR ANY PURPOSE OTHER THAN IN CONNECTION WITH A DEFINITELY GOVERNMENT-RELATED PROCUREMENT, THE UNITED STATES GOVERNMENT INCURS NO RESPONSIBILITY OR ANY OBLIGATION WHATSOEVER. THE FACT THAT THE GOVERNMENT MAY HAVE FORMULATED OR IN ANY WAY SUPPLIED THE SAID DRAWINGS, SPECIFICATIONS, OR OTHER DATA, IS NOT TO BE REGARDED BY IMPLICATION, OR OTHERWISE IN ANY MANNER CONSTRUED, AS LICENSING THE HOLDER, OR ANY OTHER PERSON OR CORPORATION; OR AS CONVEYING ANY RIGHTS OR PERMISSION TO MANUFACTURE, USE, OR SELL ANY PATENTED INVENTION THAT MAY IN ANY WAY BE RELATED THERETO.

THIS REPORT IS RELEASABLE TO THE NATIONAL TECHNICAL INFORMATION SERVICE (NTIS). AT NTIS, IT WILL BE AVAILABLE TO THE GENERAL PUBLIC, INCLUDING FOREIGN NATIONS.

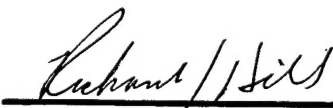
THE TECHNICAL REPORT HAS BEEN REVIEWED AND IS APPROVED FOR PUBLICATION.



RICHARD B. RIVIR  
Manager, Aerothermal Research  
Turbine Branch  
Turbine Engine Division  
Aero Propulsion & Power Directorate



CHARLES D. MACARTHUR  
Chief  
Turbine Branch  
Turbine Engine Division  
Aero Propulsion & Power Directorate



RICHARD J. HILL  
Chief of Technology  
Turbine Engine Division  
Aero Propulsion & Power Directorate

IF YOUR ADDRESS HAS CHANGED, IF YOU WISH TO BE REMOVED FROM OUR MAILING LIST, OR IF THE ADDRESSEE IS NO LONGER EMPLOYED BY YOUR ORGANIZATION PLEASE NOTIFY WL/POTT, WPAFB OH 45433-7650 TO HELP MAINTAIN A CURRENT MAILING LIST.

REPORT DOCUMENTATION PAGE			Form Approved OMB No. 0704-0188	
Public reporting burden for this collection of information is estimated to average 1 hour per response, including the time for reviewing instructions, searching existing data sources, gathering and maintaining the data needed, and completing and reviewing the collection of information. Send comments regarding this burden estimate or any other aspect of this collection of information, including suggestions for reducing this burden, to Washington Headquarters Services, Directorate for Information Operations and Reports, 1215 Jefferson Davis Highway, Suite 1204, Arlington, VA 22202-4302, and to the Office of Management and Budget, Paperwork Reduction Project (0704-0188), Washington, DC 20503.				
1. AGENCY USE ONLY (Leave blank)	2. REPORT DATE 13-16 June 1994	3. REPORT TYPE AND DATES COVERED Final 1 Nov 95 - 9 Jul 96		
4. TITLE AND SUBTITLE  The Effect of High Freestream Turbulence on Film Cooling Effectiveness		5. FUNDING NUMBERS  PE 61102F JON 2307S315		
6. AUTHOR(S)  Jeffrey P. Bons, Richard B. Rivir, Charles D. MacArthur				
7. PERFORMING ORGANIZATION NAME(S) AND ADDRESS(ES) Aero Propulsion & Power Directorate Wright Laboratory Air Force Materiel Command Wright-Patterson Air Force Base, OH 45433-7650		8. PERFORMING ORGANIZATION REPORT NUMBER		
9. SPONSORING / MONITORING AGENCY NAME(S) AND ADDRESS(ES) Aero Propulsion & Power Directorate Wright Laboratory Air Force Materiel Command Wright-Patterson Air Force Base, OH 45433-7650 POC: Richard B Rivir, WL/POTT, 513-255-5132		10. SPONSORING / MONITORING AGENCY REPORT NUMBER WL-TR-96-2097		
11. SUPPLEMENTARY NOTES				
12a. DISTRIBUTION / AVAILABILITY STATEMENT  APPROVED FOR PUBLIC RELEASE; DISTRIBUTION IS UNLIMITED		12b. DISTRIBUTION CODE		
13. ABSTRACT (Maximum 200 words) This study investigated the adiabatic wall cooling effectiveness of a single row of film cooling holes injecting into a turbulent flat plate boundary layer below a turbulent, zero pressure gradient freestream. Levels of freestream turbulence (Tu) up to 17.4% were generated using a method which simulates conditions at a gas turbine combustor exit. Film cooling was injected from a single row of five 35 degree slant-hole injectors (length/diameter = 3.5. pitch/diameter = 3.0) at blowing ratios from 0.55 to 1185 and at a nearly constant density ratio (coolant density/freestream density) of 0.95. Film cooling effectiveness data is presented for Tu levels ranging from 0.9% to 17% at a constant freestream Reynolds number based on injection hole diameter of 19000. Results show that elevated levels of freestream turbulence reduce film cooling effectiveness by up to 70% in the region directly downstream of the injection hole due to enhanced mixing. At the same time, high freestream turbulence also produces a 50-100% increase in film cooling effectiveness in the region between injection holds. This is due to accelerated spanwise diffusion of the cooling fluid, which also produces an earlier merger of the coolant jets from adjacent holes.				
14. SUBJECT TERMS			15. NUMBER OF PAGES 19	16. PRICE CODE
17. SECURITY CLASSIFICATION OF REPORT UNCLASSIFIED	18. SECURITY CLASSIFICATION OF THIS PAGE UNCLASSIFIED	19. SECURITY CLASSIFICATION OF ABSTRACT UNCLASSIFIED	20. LIMITATION OF ABSTRACT SAR	

## GENERAL INSTRUCTIONS FOR COMPLETING SF 298

The Report Documentation Page (RDP) is used in announcing and cataloging reports. It is important that this information be consistent with the rest of the report, particularly the cover and title page. Instructions for filling in each block of the form follow. It is important to *stay within the lines* to meet *optical scanning requirements*.

**Block 1. Agency Use Only (Leave blank).**

**Block 2. Report Date.** Full publication date including day, month, and year, if available (e.g. 1 Jan 88). Must cite at least the year.

**Block 3. Type of Report and Dates Covered.** State whether report is interim, final, etc. If applicable, enter inclusive report dates (e.g. 10 Jun 87 - 30 Jun 88).

**Block 4. Title and Subtitle.** A title is taken from the part of the report that provides the most meaningful and complete information. When a report is prepared in more than one volume, repeat the primary title, add volume number, and include subtitle for the specific volume. On classified documents enter the title classification in parentheses.

**Block 5. Funding Numbers.** To include contract and grant numbers; may include program element number(s), project number(s), task number(s), and work unit number(s). Use the following labels:

C - Contract	PR - Project
G - Grant	TA - Task
PE - Program Element	WU - Work Unit Accession No.

**Block 6. Author(s).** Name(s) of person(s) responsible for writing the report, performing the research, or credited with the content of the report. If editor or compiler, this should follow the name(s).

**Block 7. Performing Organization Name(s) and Address(es).** Self-explanatory.

**Block 8. Performing Organization Report Number.** Enter the unique alphanumeric report number(s) assigned by the organization performing the report.

**Block 9. Sponsoring/Monitoring Agency Name(s) and Address(es).** Self-explanatory.

**Block 10. Sponsoring/Monitoring Agency Report Number.** (If known)

**Block 11. Supplementary Notes.** Enter information not included elsewhere such as: Prepared in cooperation with...; Trans. of...; To be published in.... When a report is revised, include a statement whether the new report supersedes or supplements the older report.

**Block 12a. Distribution/Availability Statement.** Denotes public availability or limitations. Cite any availability to the public. Enter additional limitations or special markings in all capitals (e.g. NOFORN, REL, ITAR).

**DOD** - See DoDD 5230.24, "Distribution Statements on Technical Documents."

**DOE** - See authorities.

**NASA** - See Handbook NHB 2200.2.

**NTIS** - Leave blank.

**Block 12b. Distribution Code.**

**DOD** - Leave blank.

**DOE** - Enter DOE distribution categories from the Standard Distribution for Unclassified Scientific and Technical Reports.

**NASA** - Leave blank.

**NTIS** - Leave blank.

**Block 13. Abstract.** Include a brief (*Maximum 200 words*) factual summary of the most significant information contained in the report.

**Block 14. Subject Terms.** Keywords or phrases identifying major subjects in the report.

**Block 15. Number of Pages.** Enter the total number of pages.

**Block 16. Price Code.** Enter appropriate price code (*NTIS only*).

**Blocks 17. - 19. Security Classifications.** Self-explanatory. Enter U.S. Security Classification in accordance with U.S. Security Regulations (i.e., UNCLASSIFIED). If form contains classified information, stamp classification on the top and bottom of the page.

**Block 20. Limitation of Abstract.** This block must be completed to assign a limitation to the abstract. Enter either UL (unlimited) or SAR (same as report). An entry in this block is necessary if the abstract is to be limited. If blank, the abstract is assumed to be unlimited.

# DISCLAIMER NOTICE



**THIS DOCUMENT IS BEST QUALITY AVAILABLE. THE COPY FURNISHED TO DTIC CONTAINED A SIGNIFICANT NUMBER OF PAGES WHICH DO NOT REPRODUCE LEGIBLY.**



The Society shall not be responsible for statements or opinions advanced in papers or discussion at meetings of the Society or of its Divisions or Sections, or printed in its publications. Discussion is printed only if the paper is published in an ASME Journal. Papers are available from ASME for 15 months after the meeting.

Printed in U.S.A.

## THE EFFECT OF HIGH FREESTREAM TURBULENCE ON FILM COOLING EFFECTIVENESS

Jeffrey P. Bons, Charles D. MacArthur, and Richard B. Rivir  
Aero Propulsion and Power Directorate  
US Air Force Wright Laboratory  
Wright-Patterson AFB, Ohio

### ABSTRACT

This study investigated the adiabatic wall cooling effectiveness of a single row of film cooling holes injecting into a turbulent flat plate boundary layer below a turbulent, zero pressure gradient freestream. Levels of freestream turbulence ( $Tu$ ) up to 17.4% were generated using a method which simulates conditions at a gas turbine combustor exit. Film cooling was injected from a single row of five 35 degree slant-hole injectors (length/diameter = 3.5, pitch/diameter = 3.0) at blowing ratios from 0.55 to 1.85 and at a nearly constant density ratio (coolant density/freestream density) of 0.95. Film cooling effectiveness data is presented for  $Tu$  levels ranging from 0.9% to 17% at a constant freestream Reynolds number based on injection hole diameter of 19000. Results show that elevated levels of freestream turbulence reduce film cooling effectiveness by up to 70% in the region directly downstream of the injection hole due to enhanced mixing. At the same time, high freestream turbulence also produces a 50-100% increase in film cooling effectiveness in the region between injection holes. This is due to accelerated spanwise diffusion of the cooling fluid, which also produces an earlier merger of the coolant jets from adjacent holes.

### INTRODUCTION

Modern trends in aero engine gas turbine combustor design have resulted in short, high temperature rise combustors which produce highly turbulent exit flows. As combustor exit temperature is increased to benefit the engine cycle efficiency, effective film cooling of the turbine components downstream of the combustor becomes increasingly important.

Counteracting the increased heat load from the higher temperature gas by increasing the film flow is rarely an acceptable engineering solution because the coolant is usually taken from upstream in the cycle and its extraction can cause

unacceptable performance penalties. The film cooling designer is therefore faced with the challenge of obtaining the maximum efficiency from each unit of coolant flow. Accurate information on the effects of the many variables that enter the problem—pressure gradient, curvature, exit hole design, coolant and mass flow rates—is critical.

All gas turbine combustors, and in particular, the newer low aspect ratio designs produce complex exit flows which contain turbulence of varying intensity, scale, and isotropy. Recent research has shown free stream turbulence to have a significant effect on boundary layer flows. Therefore it may be expected that film cooling will also be significantly influenced by turbulence in the main stream. Although there exists a large body of film cooling effectiveness data documenting the effects of many design parameters, there have been relatively few comprehensive studies of the effect of freestream turbulence. No study to date has investigated the effect of turbulence of the type associated with gas turbine combustors on film cooling. This may be in part because, until recently, little quantitative data has been available in the open literature on combustor exit turbulence. The work of Goebel et al. (1993) and Moss and Oldfield (1991) has begun to provide details of turbulence for actual combustors. Information on many additional quantities, in particular length scales, is yet to be reported. The work of Goebel et al. found the ranges of axial and swirl turbulence intensities to be generally between 5% and 20%. Also, these values vary considerably with radial position and the amount of swirl induced in the flow by the fuel injection. Such significant intensities would be expected to greatly effect film cooling behavior. While these studies provide information on older combustor geometries, as previously noted, new combustors are shorter, with less pressure drop, and anticipated to have more severe exit turbulence.

The objective of this work is to further the understanding of how film cooling effectiveness is influenced by main stream



turbulent flow. A single row of angled injection holes is used with diameter-to-spacing and length-to-diameter ratios typical of current cooling schemes. Freestream turbulence is created by jets in cross flow, an arrangement designed to simulate the dilution jets located near or at the exit of virtually all combustors. This work concentrates on effectiveness (a measure of the mixing rate of the film with the freestream as determined from the adiabatic wall "recovery" temperature) because of its importance in most common methods of predicting gas-to-surface heat transfer.

The most comprehensive published work documenting the effects of free stream turbulence on film cooling is that of Kadotani and Goldstein (1979). These authors used turbulence generating grids in a low speed, zero pressure gradient flow to create free stream intensity fluctuations of up to about 20% and turbulent integral length scales (average eddy sizes) of 0.06 to 0.33, expressed as fractions of the film ejection hole diameter. The film cooling arrangement was a single row of angled holes similar to the present study. Kadotani and Goldstein found varying degrees of turbulence influence, which, when expressed as a ratio of disturbed effectiveness to effectiveness with a (nearly) laminar free stream, ranged from -30% to +15%. The authors concluded that three general parameters were of greatest importance in changing the effectiveness: the turbulence intensity, the blowing ratio, and the ratios of length scale to hole diameter and length scale to main stream boundary layer thickness at the hole location. All three parameters appear to alter the mixing rate between the main stream and the film coolant.

Other studies of the effect of free stream turbulence on film cooling have been presented by Jumper et al. (1989), and Brown and Saluja (1979). Jumper et al. presented effectiveness results for one nearly constant turbulence level of 16% generated using a wall jet as the mainstream flow. This turbulence level was achieved in the initial period of the wall jet velocity decay. The wall jet has velocity and turbulence profiles somewhat distinct from those of a conventional flat plate boundary layer which

makes comparison of these results to other work difficult. Nevertheless the same general trends in enhancement or decrease of effectiveness with blowing ratio as seen in Kadotani and Goldstein were observed but at a greater rate. Brown and Saluja studied film cooling from a single hole and a row of holes exiting into accelerating and decelerating flows. Freestream turbulence was generated with a grid giving levels of 1.7% and 8%. In general, increasing turbulence intensity resulted in a decrease of centerline effectiveness at all downstream locations. The spanwise averaged effectiveness values, however increased with higher Tu for blowing ratios above 0.7.

The focus of this report is the influence of turbulence intensity on film effectiveness. Turbulent length scales were measured at the film injection location and are reported. The current experiment lacks the means to independently vary this parameter. Thus the effect of length scale on effectiveness downstream of the injection point was not addressed as an independent parameter. The facility has been carefully constructed to simulate the actual turbine environment, providing, in particular, levels of free stream turbulence higher than that generated by the injected film flow in the boundary layer. When the turbulence in the freestream is greater than the turbulence in the boundary layer the transport of  $u'v'$  and  $v'T'$  throughout the boundary layer are significantly altered from the values achieved beneath a quiescent freestream. This is evidenced by the non-constant values of the Reynolds analogy factor with Tu observed in MacMullin et al. (1989) and Maciejewski and Moffat (1992). This condition, lacking in all previously published work, is necessary to properly reproduce actual engine conditions.

## EXPERIMENTAL FACILITY

The research facility used for the experiments is shown in Figure 1. The open loop wind tunnel uses a main flow blower with an external intake to provide a nominal mass flow of 1.5

## NOMENCLATURE

H	shape factor $\delta^*/\theta$
L	streamwise test section length (1.82m)
L <sub>gx</sub>	longitudinal integral length scale (cm)
L <sub>gy</sub>	vertical integral length scale (cm)
M	blowing ratio ( $\rho_{fc}U_{fc}/\rho_{fs}U_{fs}$ )
Re <sub>d</sub>	Reynolds # based on cooling hole diameter
T	static temperature
Tu	turbulence intensity ( $u'/U$ ) (%)
U	mean local streamwise velocity (m/s)
U <sub>fs</sub>	mean freestream streamwise velocity (m/s)
b	turbulence grid bar width (1.34cm)
d	film cooling hole diameter (1.905cm)
d <sub>gj</sub>	turbulence generator hole dia. (1.11cm)
dP/dx	streamwise pressure gradient (Pa/m)
u'	fluctuating streamwise velocity component
v'	fluctuating vertical velocity component
x	streamwise distance measured from downstream lip of injection hole

y	vertical distance measured from injection surface
z	spanwise distance measured from center injection hole
$\Delta_{eff}$	effectiveness deficit ( $1 - \eta_{hiTu}/\eta_{loTu}$ ) (%)
$\delta$	boundary layer thickness
$\delta^*$	boundary layer displacement thickness
$\eta$	film cooling effectiveness $(T_w - T_{aw})/(T_{fc} - T_{aw})$
$\eta_c$	centerline film cooling effectiveness
$\eta_m$	midline film cooling effectiveness
$\theta$	boundary layer momentum thickness
$\rho$	fluid density
<b>Subscripts:</b>	
aw	adiabatic wall
dTj	Reynolds # based on turbulence hole dia.
fc	in the film cooling fluid
fs	in the freestream fluid
hiTu	Tu>0.9% freestream conditions
loTu	Tu=0.9% freestream conditions
w	at the wall
$\theta$	Reynolds # based on momentum thickness



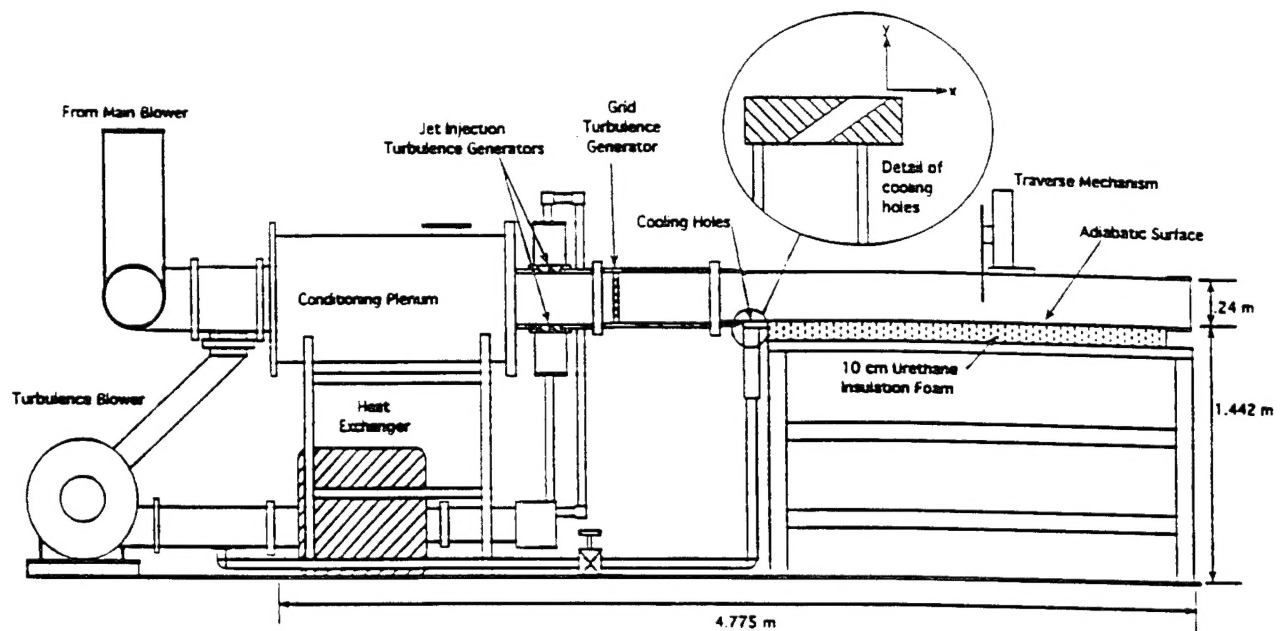


FIGURE 1: SIDE VIEW OF EXPERIMENTAL FILM COOLING FACILITY

kg/s to the test section. A heat exchanger at the main flow blower discharge can be used to vary the flow temperature from 18 to 54°C (depending on local atmospheric temperature). The main flow enters a conditioning plenum of 0.6m diameter before reaching the rectangular test section. This conditioning plenum has one layer of perforated aluminum plate followed by 7.6cm of honeycomb straightener, and 3 layers of fine screen. A circular-to-rectangular nozzle constructed of polystyrene foam conducts the flow from the 0.6m diameter plenum cross-section to the 0.24m x 0.38m test section. With this conditioning, flow uniformity of  $\pm 2.5\%$  in velocity (at  $U_{fs} = 16$  m/s) is obtained over the center 0.23m (spanwise dimension) by 0.22m (vertical dimension) of the test section (the region with coolant injection). Without employing turbulence generation devices, a freestream turbulence level of 0.9% ( $\pm 0.05$ ) was achieved over this center region.

Boundary layer bleeds are employed at the top and bottom of the test section 12.07cm upstream of the downstream lip of the film cooling injection holes (designated as  $x/d=0$  in Figures 1 & 2). At 1.22m from the plenum exit, a knife edge bleed clips off the bottom 1.27cm of the growing boundary layer. On the top of the test section (and at the same streamwise location), a circular leading edge bleeds off an additional 1.27cm of the flow, making the aspect ratio of the final test section (aspect ratio = span/height) approximately 1.76. The circular leading edge bleed is the upstream end of the adjustable top wall. The top wall pivots about this forward end in order to adjust the pressure gradient in the tunnel. For the tests presented here, constant pressure was desired and the wall was adjusted until a nondimensional pressure gradient  $(L/\rho U_{fs}^2)(dP/dx)$  of 0.0182 was achieved down the test section.

Figure 2 shows a top view of the test section indicating, boundary layer bleed, trip, film cooling holes, and thermocouple placement. At 0.64cm from the downstream lip of the coolant holes ( $x/d=0.33$ ), an adiabatic surface with imbedded thermocouples spans the 0.38m width and the 1.82m streamwise length of the test section. The surface consists of a top layer of 0.051mm thick Inconel foil epoxied to a 0.16cm thick epoxy board, which is in turn affixed to a 10cm thick insulating urethane foam. For the present experiments, no voltage potential was placed across the Inconel foils, and the surface is essentially adiabatic. The 80 (0.94mm bead diameter) iron-constantan thermocouples are mounted from the underside of the epoxy panel to within 0.051mm of the backside of the foil. The boundary layer trip is a 1.59mm diameter steel rod located at 2.54cm from the knife-edge bleed. This is approximately the height of a fictitious turbulent boundary layer starting from the knife-edge, and insures a spanwise uniform turbulent boundary layer profile at the injection point,  $x/d=0$  (9.53cm downstream of the trip).

A principal requirement of the facility is the generation of high levels of freestream turbulence. This is accomplished by two methods for the present experimental data. A 0.15m diameter "Tee" located 0.61m upstream of the inlet to the conditioning plenum leads to a bypass blower which boosts the bypass flow pressure by 7kPa. This bypass flow is then reinjected from two opposing rows of eleven 1.11cm diameter holes located on the top and bottom of the test section 1.02m upstream of the boundary layer bleed. A heat exchanger in the bypass line is used to remove the 25°C heat of compression from the bypass blower. This type of turbulence generation device was pioneered by Bogard et al. (1992), who successfully varied the velocity ratio

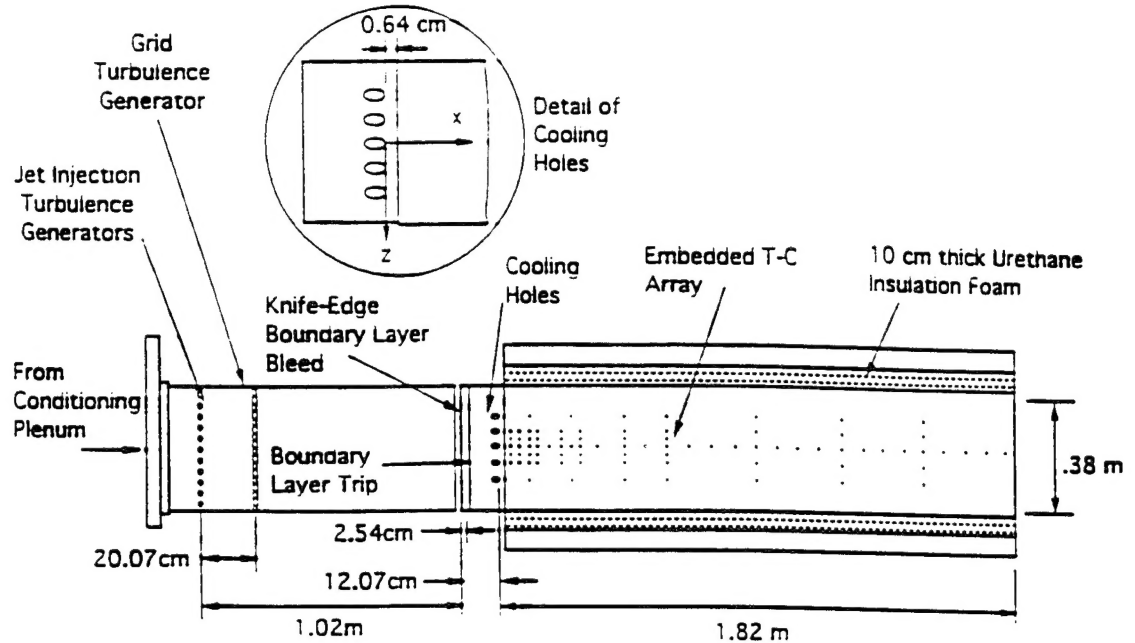


FIGURE 2: TOP VIEW OF EXPERIMENTAL FILM COOLING FACILITY

(jet velocity/freestream velocity) and the Reynolds number (based on hole diameter) to obtain uniform  $Tu$  levels from 5 to 25%.

In the present facility, a velocity ratio of 14 produced a turbulence level of 17% ( $\pm 0.85$ ) at the injection station ( $x/d_{TJ} = 103$  downstream of the turbulence generator holes). The Reynolds number based on  $d_{TJ}$  for this case is 7800 for the nominal operating conditions of  $U_{fs} = 16$  m/s in the film cooling test section. The attainable  $Tu$  level varies with both velocity ratio and  $Re_{d_{TJ}}$ , and decays down the plate slightly slower than the characteristic  $-5/7$  power law for grid-generated turbulence (Figure 4). By throttling the bypass flow down to a velocity ratio of 4.5 (and  $Re_{d_{TJ}} = 9400$ ), an 11.5%  $Tu$  level at the injection point was achieved with a uniformity of  $\pm 0.94$  in the bottom 5 cm of the flow (below  $y/d = 2.63$ ). This was considered adequate uniformity for the present study as the coolant fluid never rises above the lower 5 cm of the flow before  $x/d = 10$ , and only marginally thereafter.

To provide comparison with the bulk of elevated freestream turbulence film cooling literature which uses grid-generated turbulence, a standard square grid was installed 0.94 m upstream of the coolant injection point. The grid is made of square bars with a width of 1.34 cm and a spacing to width ratio of 4.5. The grid provided a turbulence level of 6.5% ( $\pm 0.3$ ) at the injection point. The turbulent jets and grid were never employed simultaneously. Figure 3 shows typical fluctuating velocity boundary layer profiles at the injection station for the different turbulence generation modes without film cooling injection (injection holes taped). Figure 4 shows the streamwise decay of the generated freestream turbulence (arrows denote the film cooling injection station). Boundary layer data corresponding to the four fluctuating velocity profiles in Figure 3 are tabulated in

Table 1. Turbulence levels and length scales for the freestream ( $y/d = 2.63$ ) are included in the table for comparison.

TABLE 1: CLASSIFICATION OF EXPERIMENTAL TEST CONDITIONS ( $x/d = 0$ ,  $z/d = \pm 1.5$ )

	No Turbulence Generation	Grid Generated Turbulence	Jet Generated Turbulence (Velocity Ratio = 4.5)	Jet Generated Turbulence (Velocity Ratio = 14)
<u>Data at <math>y/d = 2.6</math></u>				
$Tu$ (%)	0.96	6.76	12.01	17.3
$L_{gx}$ (cm)	6.77	3.65	6.04	7.73
<u>Data at <math>y = \delta</math></u>				
$U$ (m/s)	16.03	14.35	13.96	16.82
$Re_d$	19085	17085	16621	20026
$u'$ (m/s)	0.59	1.1	1.875	3.16
$Tu$ (%)	3.68	7.67	13.43	18.79
$L_{gx}$ (cm)	3.94	5.48	6.09	8.05
$L_{gx}/d$	2.07	2.88	3.20	4.23
$\delta$ (cm)	1.22	1.31	1.28	1.26
$\delta^*$ (cm)	0.123	0.121	0.130	0.123
$\theta$ (cm)	0.0927	0.0917	0.0991	0.0965
$H$	1.33	1.32	1.31	1.27
$\theta/d$	0.0487	0.0481	0.052	0.051
$Re_\theta$	929	822	864	1015

The source of the film cooling flow is a "Wye" located at the exit of the turbulence flow blower (and before the turbulence flow heat exchanger). The blower heat of compression provides an

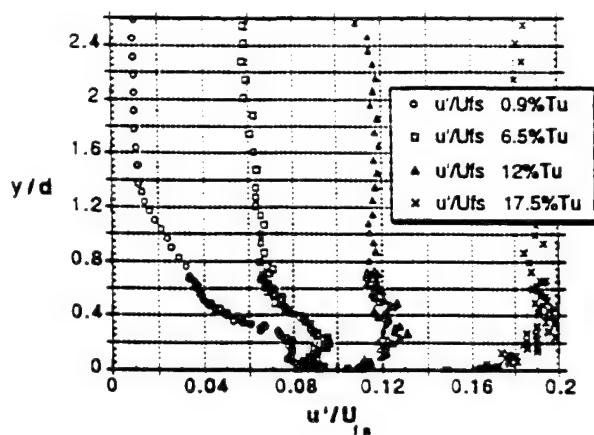


FIGURE 3: NON-DIMENSIONAL FLUCTUATING VELOCITY COMPONENT PROFILES FOR THE MAINSTREAM AT THE INJECTION POINT ( $x/d = 0$ ) WITHOUT FILM COOLING. FOUR LEVELS OF  $Tu$  SHOWN: 17.5%, 12%, 6.5%, AND 0.9%.

elevated temperature of approximately  $20^{\circ}\text{C}$  over the freestream temperature at the injection point. Due to heat loss in the film cooling flow piping, the exit temperature drops with decreasing mass flow and the temperature rise was as low as  $9^{\circ}\text{C}$  for the lowest blowing ratio tested ( $M=0.55$ ). The facility is thus run in the "film heating" vs. the "film cooling" mode with a density ratio of approximately 0.95 ("film heating" and "film cooling" are used interchangeably in this report). The row of five 1.9cm diameter injection holes is centered in the test section width. The 35 degree inclined holes are spaced at 3 hole diameters and the injection pipe length from the coolant access plenum to the exit is 3.5 hole diameters. Comparing velocity and temperature profiles from the center three holes show uniformity to within  $\pm 5\%$  nominally for both parameters.

### INSTRUMENTATION

The data presented in this report were taken using a single  $4\mu\text{m}$  diameter tungsten hot wire and an array of thermocouples. The hot wire and a flow temperature thermocouple (0.33mm bead diameter) located 0.5cm downstream (and at the same  $y$  and  $z$ ) from the hot wire probe are both mounted on a vertical traverse. A magnetically encoded linear position indicator (Sony model #SR50-030A) affixed to the traverse was used to determine the probe position to within  $2.5\mu\text{m}$ . National Instruments data acquisition and Labview software were used to acquire and process the hot wire and thermocouple voltages. Hot wire voltages were obtained using a TSI Model #IFA-100 anemometer and a National Instruments NB-MIO-16X A-to-D board. Each mean velocity measurement is obtained from the average of 1000 points taken at 200 samples per second, from which the fluctuating component of velocity,  $u'$ , was also calculated. The velocity computation algorithm corrects for local variations in

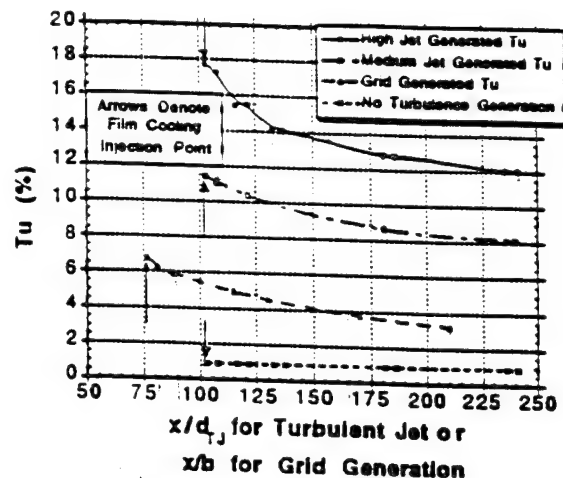


FIGURE 4: STREAMWISE DECAY OF TURBULENCE INTENSITY BEHIND TURBULENT JETS AND GRID ( $Tu$  MEASURED AT  $y/d = 2.6$ ). TURBULENT JET HOLE DIAMETER ( $d_{TJ}$ ) = 1.11cm. GRID BAR WIDTH ( $b$ ) = 1.34cm.

pressure, temperature, and humidity. Length scales were calculated by integrating to the first zero crossing of the autocorrelation coefficient function for the velocity obtained from the hot wire signal. Each length scale represents the average of 20 autocorrelations (each with 2048 velocity data points taken at 2000 samples per second). The temperature measurements were made using an integrating voltmeter with an integration period of 0.017sec for each sample.

To calculate the film effectiveness, the facility was run without film cooling to determine the adiabatic wall temperature,  $T_{aw}$ , for each setting of freestream turbulence. The film cooling fluid temperature was determined from a vertical temperature profile at  $x/d=0$  and the maximum temperature recorded was designated as  $T_{fc}$ . To determine the injection jet mean velocity a vertical velocity profile at  $x/d=0$  was integrated from the wall to the point of maximum  $u'$  (which corresponded approximately to the edge of the film cooling fluid). This average velocity,  $U$ , and the local freestream velocity,  $U_{fs}$ , were used to determine the film cooling blowing ratio.

The experimental uncertainties are calculated based on knowledge of the instrumentation used and a simple root-mean-squared error analysis (Kline and McClintock 1953). This method assumes contributions to uncertainties arise mainly from unbiased and random sources. For the film effectiveness calculation, the uncertainties in thermocouple measurements come from two distinct sources: the error of the thermocouple device and random fluctuations in the actual local temperature being sensed while at a constant operating point. The latter of these two is greater ( $\pm 0.11^{\circ}\text{C}$ ) and yields an uncertainty in  $\eta$  of  $\pm 0.008$  at  $M=1$ , and  $\pm 0.016$  at  $M=0.5$ , (using a histogram of experimental results). The insulated test surface downstream of the film cooling injection point is considered to be essentially

adiabatic. The ratio of the convective heat flux at the test surface to conduction along any path below the surface for typical flow conditions is of order 100. This indicates that the local temperature on the surface is dominated by the convection process and is an accurate indicator of film effectiveness. Uncertainty in the velocity measurement stems primarily from the calibration fit accuracy. When compared to a co-located Kiel probe velocity measurement the error is within  $\pm 1.0\%$  at flowrates of interest. Due to the 0.5cm streamwise displacement of the hot wire and the flow thermocouple, in regions of steep temperature gradients (near  $x/d=0$ ) the temperature from the thermocouple which is used in the velocity computation algorithm is as much as  $1.2^\circ\text{C}$  lower than the actual temperature at the hot wire probe. This results in a maximum additional error in  $U$  of 2% very near the injection hole (decreasing rapidly with  $x/d$ ), and was not corrected for.

## RESULTS AND DISCUSSION

The data presented in this section is divided into two subheadings. The first subheading deals with the centerline film cooling effectiveness,  $\eta_c$ , directly downstream of the injection point. Temperature and velocity (both  $U$  and  $u'$ ) profiles are used to characterize the evolving film cooling flow over first low, then high, blowing ratios. The second subheading treats the area between coolant holes, up to the point where the adjacent coolant streams merge. Together, the results explore the regions of both decreased and increased film cooling effectiveness due to high freestream turbulence.

### Effectiveness along the Hole Centerline ( $z/d = 0$ )

This research is motivated by the understanding that high levels of freestream turbulence are a reality in the environments where film cooling is used (for example: turbine airfoils and casings), and thus the interaction of freestream turbulence and film cooling should be understood. Freestream turbulence is a measure of the level of random motion of a fluid flow. It would thus be natural to expect that when elevated levels of random motion in an enclosed flow come in contact with mass injection from an adjacent surface, the injected mass will be rapidly mixed into the surrounding fluid. This first order effect would imply a reduced film cooling effectiveness for elevated levels of freestream turbulence, a result that has been reported by other researchers (namely, Kadotani and Goldstein, 1979b).

To explore the magnitude and limitations of this expected degradation in film cooling effectiveness for the current facility, wall temperature (and thus film cooling effectiveness) data were taken along the insulated surface downstream from the coolant holes. Blowing ratios from 0.55 to 1.85 were studied for four markedly different flows: (a) a quiescent (0.9%  $Tu$ ) freestream (b) 6.5% grid-generated freestream turbulence (c) 11.5% mixing jet generated freestream turbulence and (d) 17% mixing jet generated freestream turbulence. In the paper, flows are referenced by the level of  $Tu$  at the coolant injection plane, naturally this decays to lower values downstream (Figure 4).

Figure 5 shows  $\eta_c$  as a function of blowing ratio for the four different levels of freestream turbulence. Centerline effectiveness data from the middle three holes agree to within  $\pm 5\%$ , though only data for the center hole ( $z/d=0$ ) is shown. As expected, the increasing levels of  $Tu$  in the freestream generally decrease the centerline effectiveness of the cooling fluid. This decrease, or deficit (defined here as  $\Delta_{eff} = 1 - \eta_{hi}Tu/\eta_{lo}Tu$ ), reaches a maximum of 70% for  $0.55 < M < 0.95$  ( $Tu=17\%$  and  $x/d=22$ ) with the effect becoming less pronounced as  $M$  increases. The jet lift off from the cooled surface is responsible for this change in the observed deficit with higher  $M$ , and will be addressed in section B, below.

A deficit of this magnitude is considerably larger than that observed by Kadotani and Goldstein (1979b), who saw a deficit of up to 28% at  $M=0.35$  for grid generated freestream turbulence levels of 20.6%. Part of this disparity may be due to the nature of freestream turbulence generation in the two facilities. The jet generated freestream turbulence is fairly uniform through the boundary layer (Figure 3), whereas the 20.6%  $Tu$  case for Kadotani and Goldstein could only be obtained by placing the turbulence generation grid in close proximity to the film cooling injection point. This resulted in a rather non-uniform turbulence profile at  $x/d=0$ , with an actual  $Tu$  level of 12.9% at the boundary layer edge. In addition to the non-uniform vertical distribution of  $Tu$ , the axial distribution also varies rapidly with  $x$  in Kadotani and Goldstein's experiment because the injection point is still in the initial decay of the grid generated turbulence. The effectiveness deficit ( $\Delta_{eff}$ ) for the present work at a more comparable  $Tu$  level of 11.5% and at the lowest blowing ratio studied ( $M=0.55$ ) is 49%.

Another important variable in the Kadotani and Goldstein data is the vertical length scale,  $L_{gy}$ . By varying this parameter, they found that the  $\Delta_{eff}$  for 8.2% freestream turbulence with  $L_{gy}=0.39\text{cm}$  was comparable to the  $\Delta_{eff}$  for the 12.9% turbulence with  $L_{gy}=0.07\text{cm}$  quoted above, at a constant blowing ratio. This demonstrates the importance of turbulent length scale in completely characterizing the effect of freestream turbulence on film cooling effectiveness. By comparison, in the present study the longitudinal length scale for the jet generated turbulence is 50% larger than the scale of the 6.5% grid generated turbulence in the boundary layer. This difference grows to as large as 110% at  $y/d=2.63$ , Table 1. This "larger" jet turbulence scale may contribute to larger  $\Delta_{eff}$  with high levels of freestream turbulence in the present study. No definitive conclusions can be reached with the present data, though, since turbulence scale and intensity were not varied independently. Other factors contributing to the difference in results will be discussed in the succeeding sections.

**A) Low Blowing Ratios ( $0.5 < M < 0.95$ ).** Han and Mebendale (1986) reported the optimum blowing ratio range to be from 0.5 to 0.7 ( $x/d \leq 20$ ) for single row film cooling at a Reynolds number based on hole diameter of 20000. The Reynolds number of the data presented here is approximately the same (19000), and so it is instructive to compare the optimum blowing ratio and the effect of freestream turbulence. From

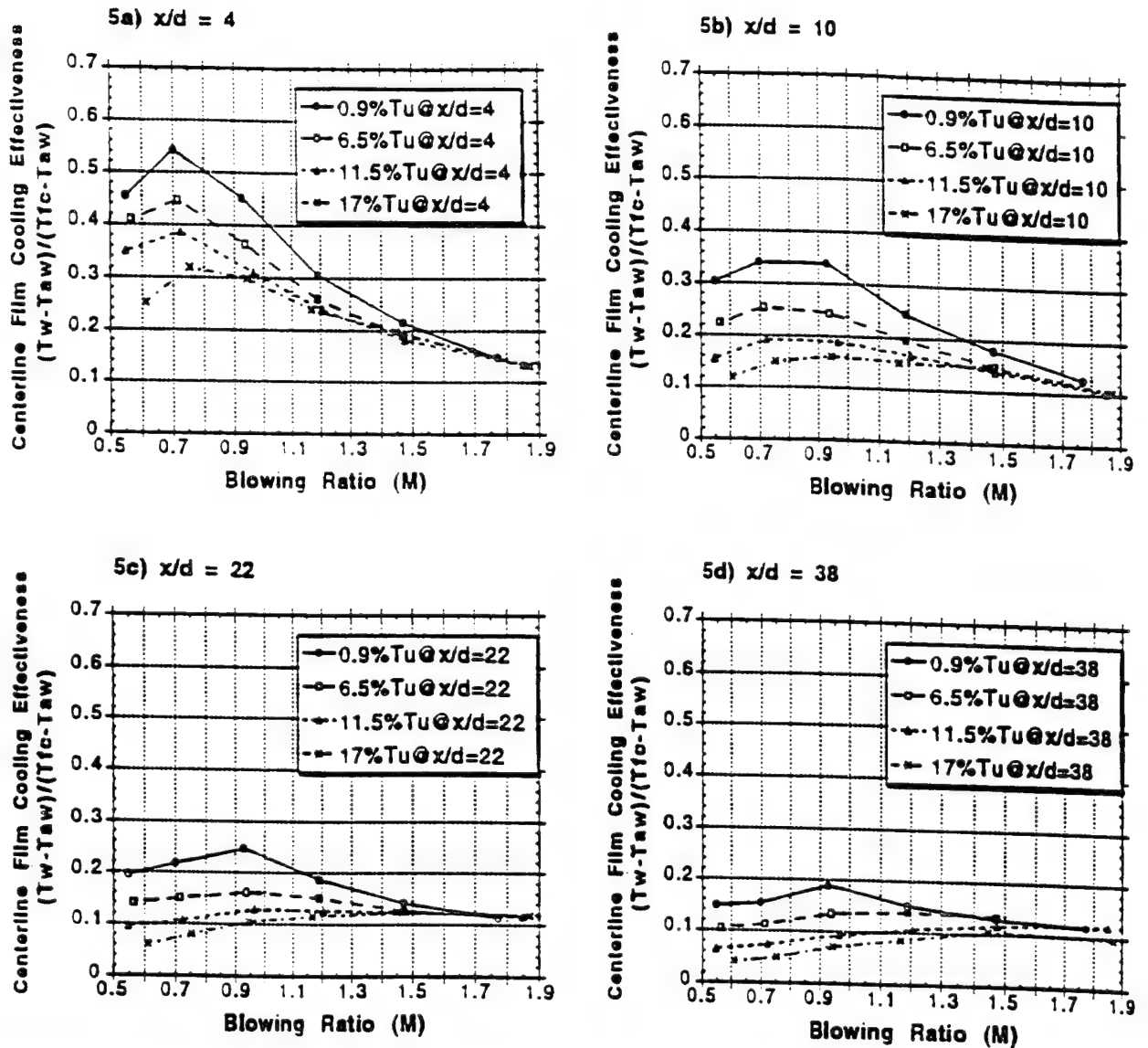


FIGURE 5a-d: CENTERLINE FILM COOLING EFFECTIVENESS AT FOUR DIFFERENT  $x/d$  STATIONS: 4, 10, 22, & 38. ( $z/d = 0$ ). DATA FOR FOUR LEVELS OF  $Tu$ : 17%, 11.5%, 6.5%, AND 0.9%.  $U_{fs} = 16$  m/s ( $Re_d = 19000$ ).

Figure 5, though the data is not sufficient to determine precisely, it appears that the optimum  $M$  shifts to higher  $M$  as  $Tu$  increases. The elevated turbulence also appears to flatten the region of optimum effectiveness, resulting in a considerably wider range of blowing ratios over which the effectiveness remains within a 10% band of the optimum effectiveness point.

In this range of blowing ratios ( $0.55 < M < 0.95$ ), before blow-off becomes a significant factor, film cooling effectiveness decreases monotonically with freestream turbulence. A rudimentary attempt to correlate the loss in effectiveness to the  $Tu$  level at the point of injection results in the following empirical form:

$$\Delta_{eff} = \left( 1 - \frac{\eta_{hi} Tu}{\eta_{lo} Tu} \right) = B(1 - \exp(-m \frac{x}{d}))(1 - \exp(-n Tu)) \quad [Tu \text{ in } \%]$$

where  $n$  and  $B$  are functions of blowing ratio. Values of  $B=1.05$ ,  $m=0.5$ , and  $n=0.05$  fit the data presented in this paper for  $x/d \leq 38$  and  $0.55 < M < 0.95$  to within  $\pm 17\%$ . The form of this expression is intuitive, and without physical basis. Though the empirical expression implies that  $Tu$  is the only parameter that influences effectiveness, other characteristics of the freestream turbulence generated for the different cases presented here (for example, integral length scale) may play a significant role in effectiveness.



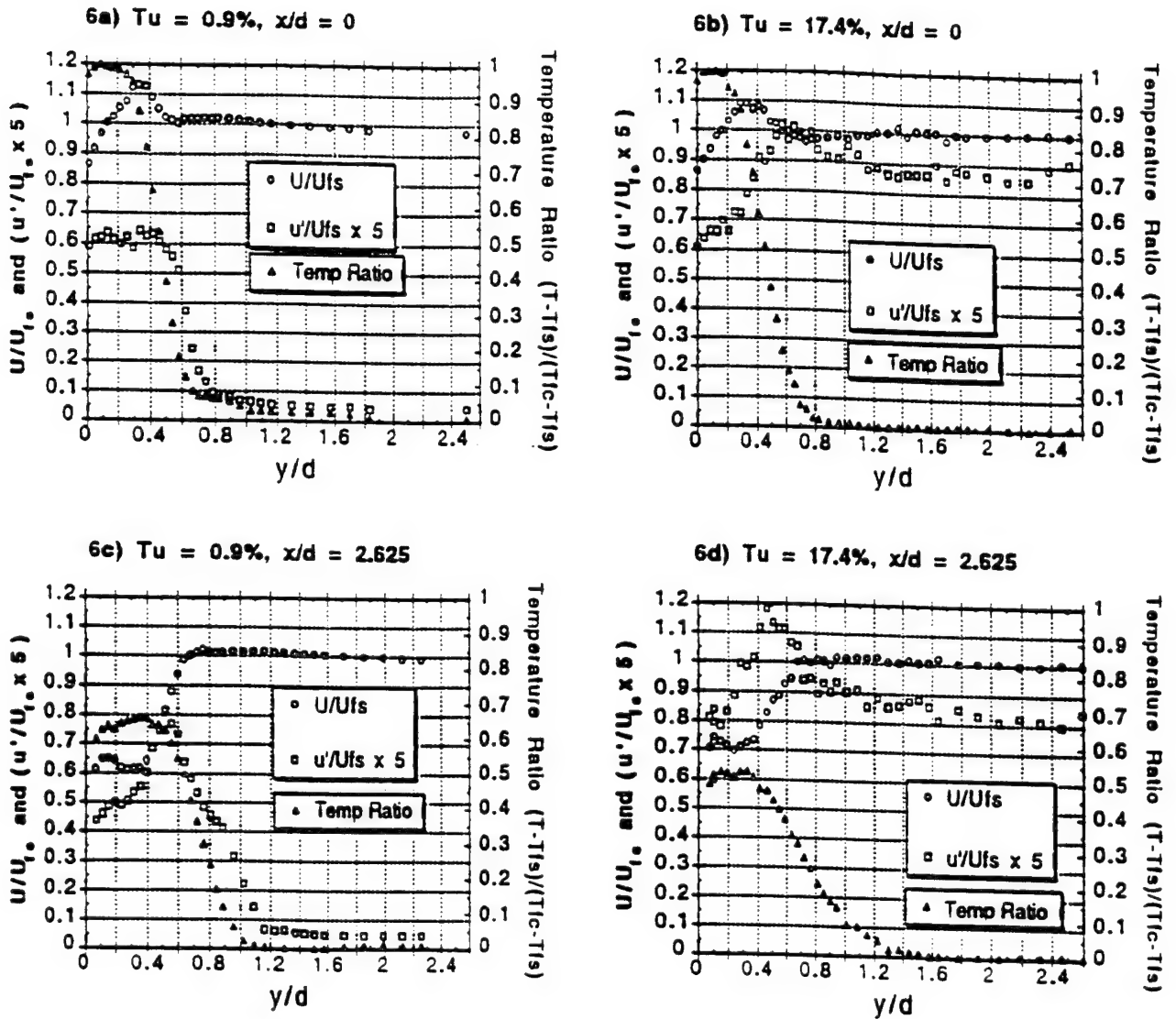


FIGURE 6a-d:  $U/U_{fs}$ ,  $u'/U_{fs}$ , AND TEMPERATURE RATIO BOUNDARY LAYER PROFILES AT TWO  $x/d$ : 0 & 2.625 ( $z/d = 0$ ). DATA FOR  $Tu = 0.9\%$  &  $M = 0.99$  COMPARED TO  $Tu = 17.4\%$  &  $M = 0.95$ .

reductions. Notably, it is evident from Figure 5 that film cooling effectiveness data based solely on grid generated turbulence (with its inherent maximum of uniform  $Tu \approx 8\%$ ) would be inadequate for predicting the trend at high  $Tu$  levels ( $Tu > 10\%$ ) accurately. This is the fundamental reason for the development of the present experimental facility.

To understand the underlying reason for the loss in cooling effectiveness with increasing  $Tu$ , it is instructive to examine temperature and velocity (mean and fluctuating components) boundary layer profiles at various  $x/d$  locations downstream of the injection hole. Figures 6a-h show these profiles at four  $x/d$  stations for  $M=0.95$  and two  $Tu$  levels (0.9% and 17.4%).  $U$  and  $u'$  are non-dimensionalized by the freestream mean velocity  $U_{fs}$ .

The static temperature is shown as a ratio of the difference between local temperature and freestream temperature and the difference between the film cooling temperature and the freestream temperature. The non-dimensional fluctuating velocity component,  $u'/U_{fs}$ , is shown with a factor of 5 to facilitate presentation on the same scale with the non-dimensional mean velocity.

Of particular note is the slanted shape of the coolant fluid velocity profile in both cases (see the  $y/d < 0.4$  region of velocity profiles on figures 6a & b). This non-parabolic shape is discussed in detail by Leylek and Zerkle (1993) and is due to the flow internal to the film cooling hole and access plenum. Separation off the downstream edge at the inlet to the film cooling injection

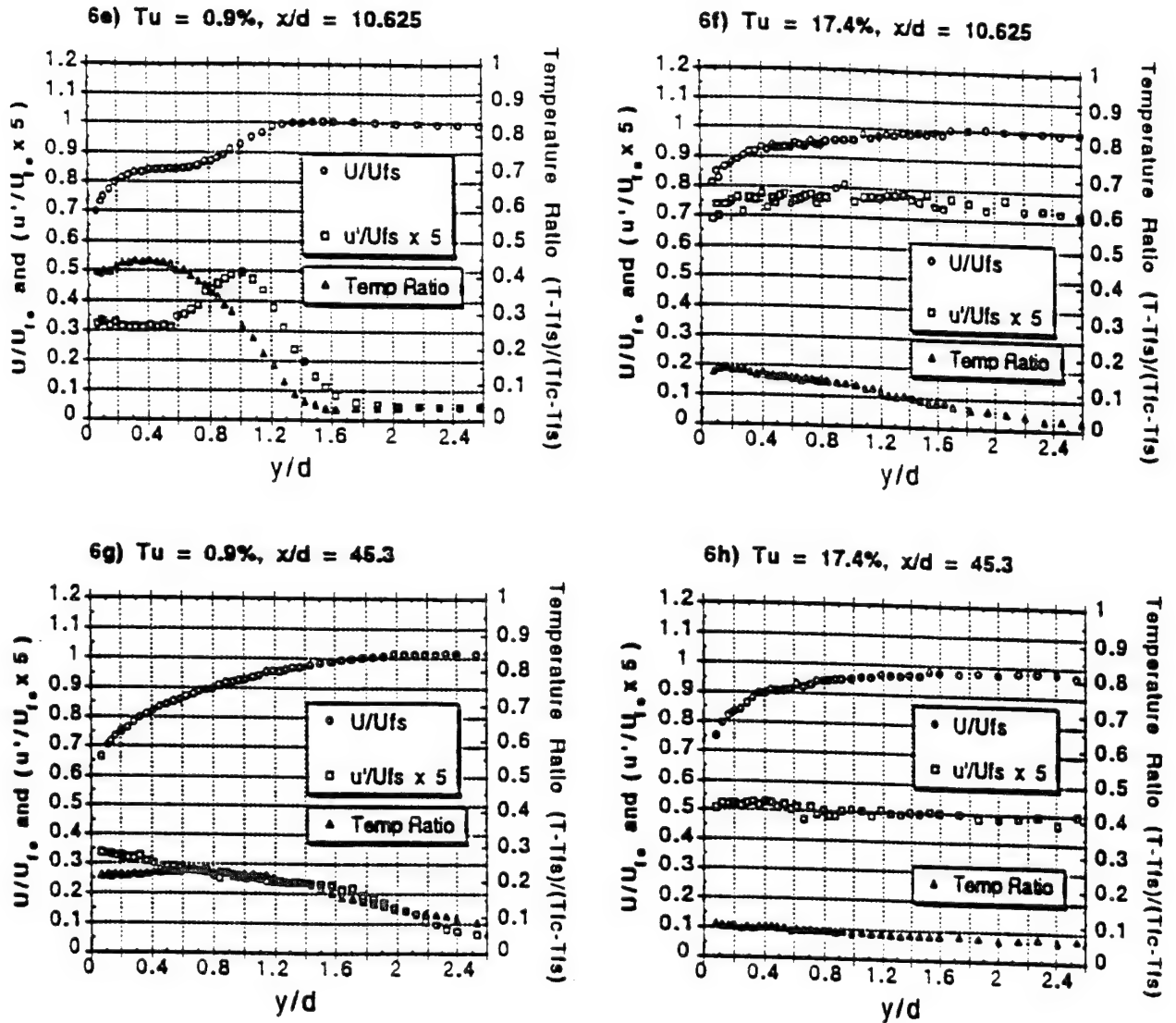


FIGURE 6e-h:  $U/U_{fs}$ ,  $u'/U_{fs}$ , AND TEMPERATURE RATIO BOUNDARY LAYER PROFILES AT TWO  $x/d$ : 10.625 & 45.3 ( $z/d = 0$ ). DATA FOR  $Tu = 0.9\%$  &  $M = 0.99$  COMPARED TO  $Tu = 17.4\%$  &  $M = 0.95$ .

tube causes the fluid to hug the upstream wall of the tube. For tubes with short  $L/d$ , representative of modern film cooling applications, the flow has insufficient length to establish a traditional pipe flow velocity profile, resulting in a skewed velocity profile at exit. This effect brings the injected momentum apex further away from the wall and closer to the high  $Tu$  freestream. In the presence of elevated freestream turbulence, this unique feature of short  $L/d$  cooling tubes could result in a larger  $\Delta_{eff}$  than for cooling injected with long  $L/d$  tubes. Since the momentum core is closer to the turbulent shear layer and the freestream, it may experience an accelerated dissipation compared to the long  $L/d$  case where the velocity profile is more symmetric. This effect may help to partly explain the lower  $\Delta_{eff}$

values observed by Kadotani and Goldstein (1979b), who used a facility with  $L/d=62$  compared to  $L/d=3.5$  in the present facility. Exit velocity profiles taken at  $M=0.55$  and  $M=1.87$  show the "skewness" of this film cooling velocity profile to increase with  $M$  (also noted by Leylek and Zerkle, 1993).

Proceeding downstream from the injection location (Figures 6c-h), significant differences develop between the high and low  $Tu$  flows. For the low  $Tu$  case, the film cooling fluid and the freestream merge in a strong shear region located at approximately  $y/d=0.5$  from the wall. Below this shear region, the fluctuating velocity component of the film cooling flow is remarkably flat, with the maximum of  $(u'/U_{fs} \times 5) = 0.6$  at  $x/d=0$  decaying rapidly (with a nearly linear decay rate of 4.4 [m/s]/m



from  $x/d=0$  to  $x/d=10$ ) with  $x/d$  due to the strong damping effect of the surrounding quiescent freestream. The diffusion of the thermal energy in the film cooling flow is also retarded by the relatively inactive freestream, and the temperature profile retains its shape (and thus effectiveness) well beyond  $x/d=20$ .

The situation is markedly different in the high Tu case, where the formation of two distinct flow regimes is impeded immediately by a high level of mixing. At the injection plane ( $x/d=0$ ), the peak velocity of the injected fluid is reduced from  $U/U_{fs} = 1.12$  for low Tu to  $U/U_{fs} = 1.09$  for high Tu. The  $u'$  level in the film cooling fluid rises dramatically from a value of  $(u'/U_{fs} \times 5) = 0.6$  at the wall to  $(u'/U_{fs} \times 5) = 1.0$  at the velocity peak. Of greater concern for effectiveness, the temperature profile at  $x/d=0$  is already partially dissipated. The maximum temperature begins to drop at  $y/d=0.17$  for the high Tu case vs.  $y/d=0.27$  for the low Tu case. This lower temperature in the shear region is indicative of heightened mixing with the freestream. By  $x/d=2.6$ , the film cooling flow for the high Tu case has lost 48% of its effectiveness vs. 34% for the low Tu case. The original freestream velocity profile recovers quickly from the disruption caused by the mass injection and by  $x/d=10.6$  there is little trace of the film cooling fluid ( $u'/U_{fs}$  is nearly constant down to the wall).

In summary, freestream turbulence has a profound mixing effect resulting in accelerated break-up of the injected film cooling flow. This is the underlying cause of the loss of centerline effectiveness. The trends in Figures 6a-b are similar for the two intermediate levels of Tu, though less pronounced.

**B) High Blowing Ratios ( $M > 0.95$ ).** From Figure 5, it is evident that the loss in  $\eta_c$  due to high freestream turbulence becomes less pronounced as M increases. This is due to the film cooling fluid's separation from the surface (blow-off). This blow-off is well documented in the literature, but little has been reported on the effect of elevated freestream turbulence on the blow-off phenomenon. For  $M=1.5$ , Kadotani and Goldstein (1979b) reported that  $\eta_c$  increased everywhere with elevated freestream turbulence. By comparison, high freestream turbulence levels appear to have two noteworthy influences on the separated film cooling flow in this study. Figure 7 is a close-up of  $\eta_c$  vs.  $x/d$  for  $M=1.47$  and two different Tu levels. As shown, the first several wall thermocouples exhibit a rising temperature with  $x/d$  and then fall off as expected after reaching a maximum at  $x_1$  and  $x_2$  (for the high and low Tu cases respectively). This region of positive  $dT/dx$  is indicative of separated film cooling fluid which is gradually reattaching to the wall. From the distances noted on Figure 7 ( $x_2 > x_1$ ), it is clear that higher freestream turbulence lessens the streamwise extent of the initial blow-off region.

This observation is supported by Figure 8's mean velocity and temperature profile data at  $x/d=0$  and 2.625 for two levels of Tu and  $M=1.47$ . As shown, the elevated Tu of the surrounding fluid rapidly diffuses the injected coolant fluid, dropping the peak in U

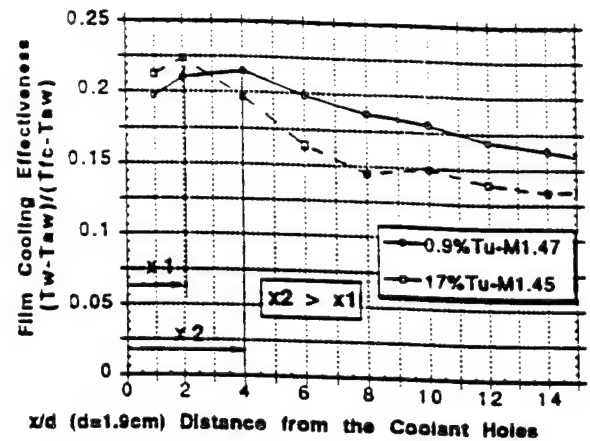
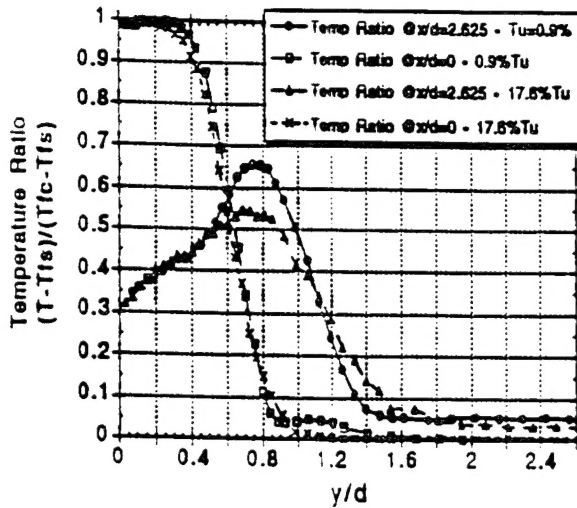


FIGURE 7: CENTERLINE FILM COOLING EFFECTIVENESS FOR TWO LEVELS OF Tu: 17.0% AND 0.9% (BLOWING RATIOS OF 1.45 & 1.47 RESPECTIVELY).  $U_{fs}=16\text{m/s}$  ( $Re_d=19000$ ) CLOSE-UP OF BLOW-OFF REGION FOR  $z/d=0$ .

and T dramatically as the flow progresses from  $x/d=0$  to 2.625. By conservation of energy, this lost thermodynamic energy must be transported elsewhere in the flow, and (as will be discussed in the succeeding section) a significant amount mixes laterally. Some of the energy also appears to mix vertically, as is evidenced by the slightly higher T and U for high Tu vs. low Tu above and below the greatly reduced peak ( $x/d=2.625$ ). The vertical diffusion caused by the high freestream turbulence brings the film cooling fluid in contact with the surface more quickly than for the case with low Tu. Though the fluid which comes in contact with the wall is at a lower, mixed-out temperature, the contact is made at a smaller  $x/d$  (approximately  $x/d=2$ ) in the presence of 17% Tu vs. the 0.9% Tu case ( $x/d=4$ , Figure 7).

The second effect of elevated freestream turbulence on film cooling blow-off is apparent beyond  $x/d=30$  on Figure 9, which shows the centerline effectiveness down the adiabatic surface for four turbulence levels and two blowing ratios:  $M=0.75$  (minimal blow-off) and  $M=1.5$  (significant blow-off). Looking closely at the  $M=1.5$  plot, a significant change in the  $\eta_c$  trend with  $x/d$  is detected at  $x/d=15$ . Upstream of this location, the low Tu  $\eta_c$  data are clearly superior. After  $x/d=15$ , the  $\eta_c$  decay with  $x/d$  is arrested for the  $Tu=6.5\%$  case, and  $\eta_c$  remains essentially flat thereafter. Figure 10 compares the centerline and midline effectiveness data for high and low turbulence at  $M=0.75$  and 1.2. From this figure it is clear that the point of spanwise film uniformity (adjacent stream merger) occurs at approximately  $x/d=10$  for high Tu vs. beyond  $x/d=30$  for low Tu. The change in  $\eta_c$  decay rate noted in Figure 9b at  $x/d=15$  is due to this earlier merger of the adjacent cooling jets for high Tu. After the merger, the film is essentially spanwise uniform. Without any further spanwise dissipation due to high freestream turbulence, the  $\eta_c$  decay flattens for  $Tu=6.5\%$ . The merger doesn't occur for the low Tu flow before  $x/d=30$ , and a slow  $\eta_c$  decay continues well down

8a) Temperature Ratio for  $Tu=0.9\%$  &  $17.6\%$  at  $x/d=0$  &  $2.625$



8b)  $U/U_{fs}$  for  $Tu=0.9\%$  &  $17.6\%$  at  $x/d=0$  &  $2.625$

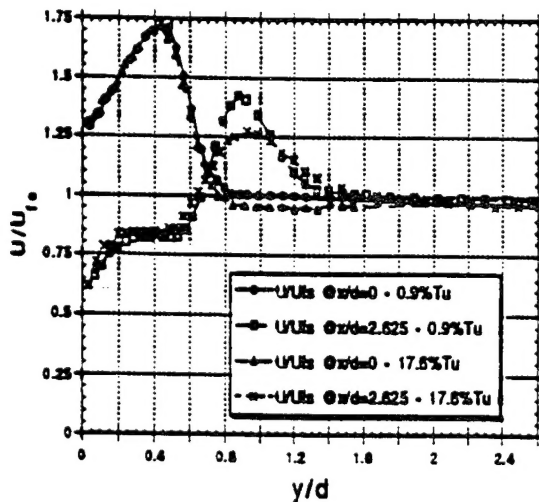
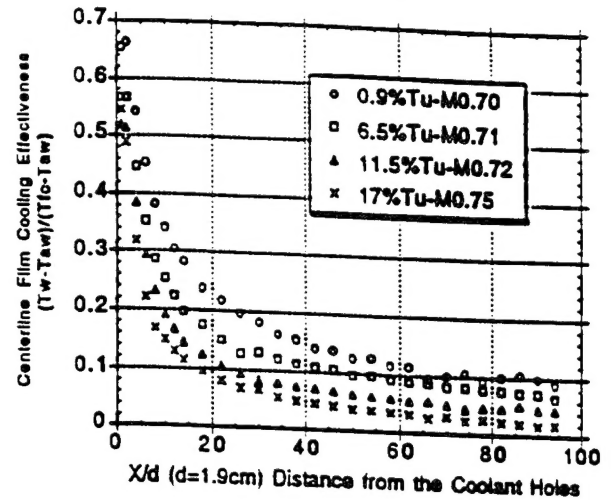


FIGURE 8a&b: TEMPERATURE RATIO AND  $U/U_{fs}$  BOUNDARY LAYER PROFILES AT TWO  $x/d$  STATIONS: 0 & 2.625 ( $z/d=0$ ). DATA SHOWN FOR  $Tu=0.9\%$  &  $M=1.47$  vs.  $Tu=17.6\%$  &  $M=1.45$ .

the adiabatic surface for this case. The accelerated spanwise diffusion caused by high freestream turbulence makes the coolant "more effective" beyond  $x/d=30$  for the  $Tu=6.5\%$  case. A similar change in  $\eta_c$  decay is noted at  $x/d=15$  for the two higher  $Tu$  levels of  $11.5\%$  and  $17\%$ . These higher levels create enough vertical dissipation beyond this point to continue decreasing the cooling effectiveness with  $x/d$  (unlike the  $\eta_c$  for  $Tu=6.5\%$ , which

9a) Blowing Ratio = 0.75



9b) Blowing Ratio = 1.5

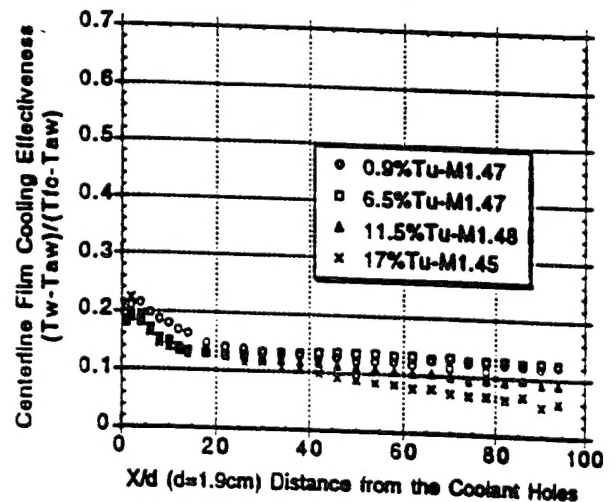


FIGURE 9a&b: CENTERLINE FILM COOLING EFFECTIVENESS VS.  $x/d$  FOR TWO BLOWING RATIOS ( $M=0.75$  &  $1.5$ ) AND FOUR FREESTREAM TURBULENCE LEVELS:  $17.0\%$ ,  $11.5\%$ ,  $6.5\%$ , AND  $0.9\%$ .  $U_{fs}=16$  m/s ( $Re_d=19000$ ),  $z/d=0$ .

is flat). There appears to be an optimum level of  $Tu$  for this unexpected effectiveness enhancement at large  $x/d$ .

#### Effectiveness along the Hole Midline ( $z/d=1.5$ )

The previous data have documented the behavior of the film cooling fluid directly downstream of the injection hole ( $z/d=0$ ). These data are representative of the spanwise average

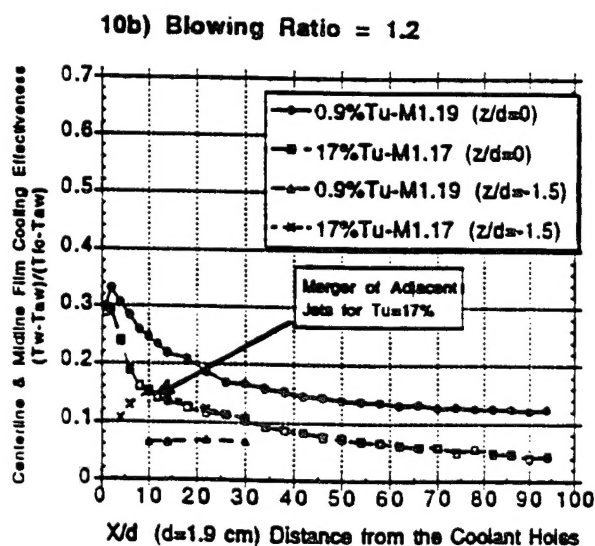
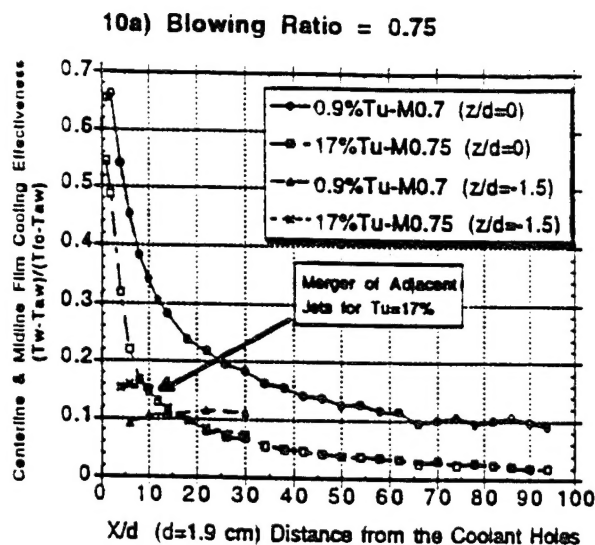


FIGURE 10a&b: CENTERLINE & MIDLINE FILM COOLING EFFECTIVENESS ( $z/d = 0$  &  $-1.5$ ) vs.  $x/d$  FOR 2 BLOWING RATIOS: 0.75 & 1.2. DATA FOR  $Tu = 0.9\%$  &  $17.0\%$ .  $U_{fs} = 16$  m/s ( $Re_d = 19000$ )

effectiveness downstream of the point at which the adjacent streams merge. The point of spanwise uniformity (stream merger) is, however, greatly dependent on the level of freestream turbulence in the surrounding fluid (as noted earlier from Figure 10). The effect of freestream turbulence on the effectiveness of film cooling fluid between the coolant holes is of equal interest to the designer.

Figure 11 shows data obtained from the surface thermocouples located exactly between the center cooling hole and its  $-z$

neighbor (the  $z/d=+1.5$  and  $z/d=-1.5$  data agree to within  $\pm 4\%$  nominally, but only the  $-z$  data are shown as the  $\eta_c$  data from the  $-z$  hole are closest to the  $\eta_c$  data from the center hole). The data are presented in a format identical to that in Figure 5, though at  $x/d$  locations of 6, 14, & 30. Except at very low blowing ratios, the elevated freestream turbulence data show a greatly improved effectiveness, even as far down the surface as  $x/d=30$  for some high blowing ratios. Brown and Saluja (1978) also observed an increase in midline effectiveness with increased  $Tu$ . The mixing of film cooling fluid which resulted in a dramatically reduced  $\eta_c$  has brought some of that effectiveness spanwise. By conservation of energy,  $\eta_m$  is enhanced by the high turbulence in the freestream, up to 100% at  $M=1.5$  and  $x/d=14$ . The data also reveal the complexity of the effects that freestream turbulence has on  $\eta_m$  in that the observed effect is not always monotonic with  $Tu$ . For example, in Figure 11a the 6.5%  $Tu$  data are more effective than the 11.5% data at low blowing ratios. In Figure 11b, the  $Tu=6.5\%$  data are most effective for low blowing ratios while the  $Tu=17\%$  data are best at high blowing ratios. Also, at  $x/d=30$  (Figure 11c), the  $Tu=6.5\%$  data are superior for low blowing ratios while the  $Tu=11.5\%$  data are best at high blowing ratios. The characteristics of turbulence that are responsible for these "inconsistencies" are not fully understood, although comparisons of integral length scale provide some additional insight.

The measured length scale of the grid generated turbulence given in Table 1 is considerably smaller than the jet generated length scales and approximately equal to the distance between adjacent holes ( $L_{gx}/d=2.88$  vs. hole spacing/ $d = 3$ ). Though this is a streamwise length scale, the associated spanwise length scale will also be relatively "smaller" than in the jet generated case, and may be better suited to dissipating the film fluid laterally. Kadotani and Goldstein (1979a) also reported a greater lateral spread of cooling fluid for "smaller" scale vs. "larger" scale freestream turbulence. Figure 12 presents the Figure 11 data in an  $\eta_m$  vs.  $x/d$  format and shows the same trends more clearly (data for  $M=0.75$  and 1.2 only). Clearly, there is some optimization of  $M$ ,  $Tu$ , and possibly  $L_{gx}/d$  that must be performed by the turbine designer to achieve a unique design requirement.

## SUMMARY AND CONCLUSIONS

Effectiveness data has been presented for a practical range of blowing ratios and four levels of freestream turbulence. Markedly different results are obtained for effectiveness directly in line with the coolant holes compared to effectiveness in the space between adjacent coolant holes, with a strong dependence on blowing ratio. It appears that the simple conclusion "high freestream turbulence decreases the effectiveness of discrete hole film cooling" is not altogether correct. Figure 10 summarizes the composite result for effectiveness at both spanwise locations, comparing the effect of 0.9%  $Tu$  to 17%  $Tu$  at  $M=0.75$  and 1.2. Freestream turbulence drastically reduces the effectiveness of film cooling directly behind the injection holes at low to moderate blowing ratios. At high blowing ratios, however, freestream

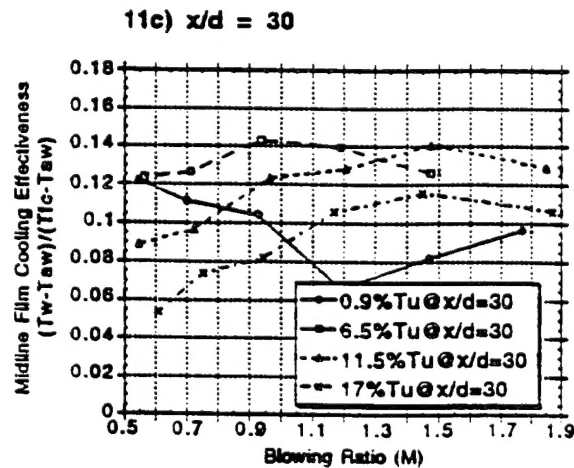
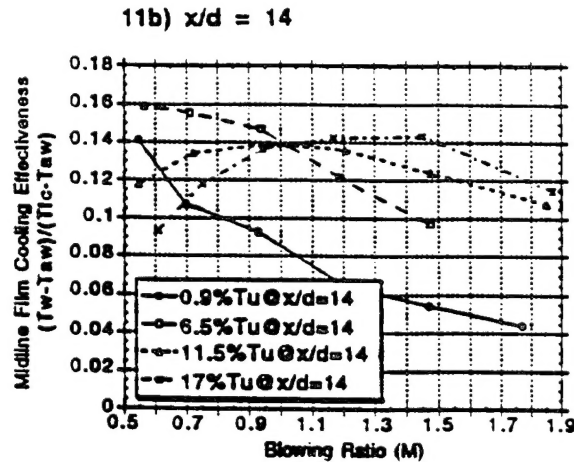
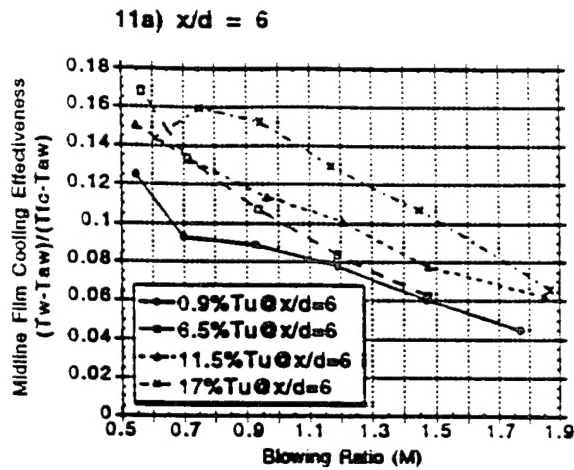


FIGURE 11a-c: MIDLINE FILM COOLING EFFECTIVENESS ( $z/d = -1.5$ ) AT 3  $x/d$ : 6, 14, & 30. DATA FOR 4 LEVELS OF  $Tu$ : 0.9%, 6.5%, 11.5%, AND 17.0%.  $U_{fs} = 16$  m/s ( $Re_d = 19000$ )

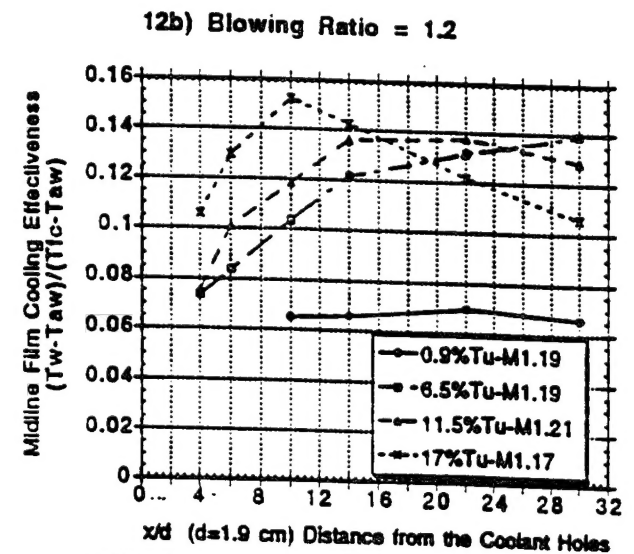
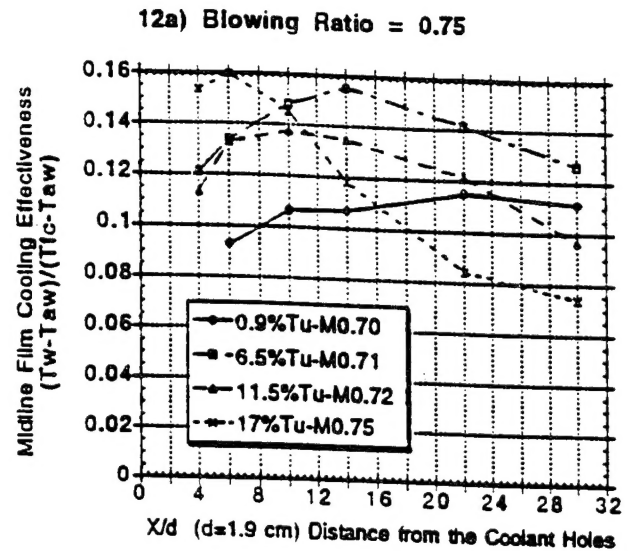


FIGURE 12a&b: MIDLINE FILM COOLING EFFECTIVENESS ( $z/d = -1.5$ ) VS.  $x/d$  FOR TWO BLOWING RATIOS: 0.75 & 1.2. DATA FOR 4 LEVELS OF  $Tu$ : 0.9%, 6.5%, 11.5%, AND 17.0%.  $U_{fs} = 16$  m/s ( $Re_d = 19000$ )

turbulence reduces the extent of blow-off, and diffuses the separated fluid down to the wall more quickly, resulting in higher effectiveness for  $x/d > 30$ . Also, the diffusion of coolant fluid with high  $Tu$  results in a dramatic increase in the lateral spread of the adjacent streams. High  $Tu$  creates a more uniform film more quickly and increases the resulting effectiveness between the coolant holes. Changes in effectiveness by a factor of two (both up and down) at practical values of blowing ratio, and over

significant regions, are documented for  $Tu$  in the range from 0.9% to 17%. An empirical correlation is offered that predicts the centerline effectiveness deficit for high turbulence levels to a reasonable degree of accuracy. However, this correlation does not include the effects of such additional variables as turbulent length scales, streamwise pressure gradient, and curvature. The influences of these parameters have not been investigated or documented at the present time. Future plans include parametric studies of these variables also.

The density ratio between the coolant and the freestream was held constant throughout this study at approximately 0.95. In typical turbine engine applications, the film cooling fluid is at times 500°C cooler than the core flow, with a density ratio of 1.5 to 2.0. Investigations by Goldstein et al. (1974) and Sinha et al. (1990) show that centerline film cooling effectiveness generally increases with higher density ratio for the same blowing ratio ( $M$ ). This trend is more evident at higher blowing ratios,  $M > 0.7$ . There is still considerable discussion over the mechanism for this influence and the effect of elevated freestream turbulence has not been investigated. The authors intend to make this an area of future research.

In summary, freestream turbulence is an important flow parameter that must be properly understood and simulated to design appropriate film cooling flows for a given application. From the data presented, it appears that certain features of cooling flows (blowing ratio, diameter, spacing/d,  $L/d$ ) can be tailored to optimize film cooling effectiveness for a given turbulent environment.

## ACKNOWLEDGMENTS

The authors wish to recognize the assistance and expert craftsmanship of the Aeronautical Systems Center's Development, Manufacturing, and Modification Facility (Zone Shop 1), specifically Mr. Larry Foland and Mr. Jerry Reed, for the construction of the test facility. Also, we would acknowledge the professional advice and assistance offered by the other members of the Wright Laboratory Aerothermal Research team: namely Mr. Gregory Cala, Mr. Edward Michaeis, Mr. David Pestian, and Dr. Shichuan Ou. This work was performed under partial sponsorship from the Air Force Office of Scientific Research. Dr. James McMichael is the project manager.

## REFERENCES

- Bogard, D.G., Thole, K.A., and Crawford, M.E., 1992, "Hydrodynamic Effects on Heat Transfer for Film-Cooled Turbine Blades", Technical Report No. WL-TR-92-2035, U.S. Air Force Wright Laboratory, Wright-Patterson AFB, OH.
- Brown, A., and Saluja, C.L., 1979, "Film Cooling from a Single Hole and a Row of Holes of Variable Pitch to Diameter Ratio", *Int. J. Heat and Mass Transfer*, Vol. 22, pp 525-533.
- Goebel, S. G., Abuaf, N., Lovett, J. A., and Lee, C.-P., 1993, "Measurements of Combustor Velocity and Turbulence Profiles", ASME Paper 93-GT-228.
- Goldstein, R. J., Eckert, E. R. G., and Burggraf, F., 1974, "Effects of Hole Geometry and Density on Three-Dimensional Film Cooling", *Int. J. Heat and Mass Transfer*, Vol. 17, pp 595-607.
- Han, J. C., and Mehendale, A. B., 1986, "Flat Plate Film Cooling With Steam Injection Through One Row and Two Rows of Inclined Holes", *ASME Journal of Turbomachinery*, Vol. 108, pp. 137-144.
- Jumper, G.W., Elrod, W.C., and Rivir, R.B., 1991, "Film Cooling Effectiveness in High-Turbulence Flow", *ASME Journal of Turbomachinery*, Vol. 113, pp 479-483.
- Kadotani, K., and Goldstein, R. J., 1979a, "On the Nature of Jets Entering a Turbulent Flow Part A - Jet-Mainstream Interaction", *ASME Journal of Engineering for Power*, Vol. 101, pp. 459-465.
- Kadotani, K., and Goldstein, R. J., 1979b, "On the Nature of Jets Entering a Turbulent Flow Part B - Film Cooling Performance", *ASME Journal of Engineering for Power*, Vol. 101, pp. 466-470.
- Kline, S. J., and McClintock, F. S., Jan 1953, "Describing Uncertainties in Single-Sample Experiments", *Mechanical Engineering*, pp 3-8.
- Leylek, J. H., and Zerkle, R. D., 1993, "Discrete-Jet Film cooling: A Comparison of Computational Results with Experiments", ASME Paper 93-GT-207.
- Maciejewski, P. K., and Moffat, R. J., Nov 1992, "Heat Transfer with Very High Free-Stream Turbulence: Part II - Analysis of Results", *ASME Journal of Heat Transfer*, Vol. 114, pp. 834-839.
- MacMullin, R., Elrod, W., and Rivir, R., Jan 1989, "Free-Stream Turbulence From a Circular Wall Jet on a Flat Plate Heat Transfer and Boundary Layer Flow", *ASME Journal of Turbomachinery*, Vol. 111, pp. 78-86.
- Moss, R. W., and Oldfield, M. L. G., 1991, "Measurements of Hot Combustor Turbulence Spectra", ASME Paper 91-GT-351.
- Sinha, A. K., Bogard, D. G., and Crawford, M. E., 1990, "Film Cooling Effectiveness Downstream of a Single Row of Holes with Variable Density Ratio", ASME Paper 90-GT-43.